# Fuzzy-superpixels for Polarimetric SAR Images Classification

Yuwei Guo, *Student Member, IEEE,* Licheng Jiao, *Fellow, IEEE,* Shuang Wang, *Member, IEEE,* Shuo Wang, *Member, IEEE,* Fang Liu, *Senior Member, IEEE,* and Wenqiang Hua

***Abstract*—Superpixels technique has drawn much attention in computer vision applications. Each superpixels algorithm has its own advantages. Selecting a more appropriate superpixels algorithm for a specific application can improve the performance of the application. In the last few years, superpixels are widely used in polarimetric synthetic aperture radar image classification. However, no superpixel algorithm is especially designed for image classification. It is believed that both mixed superpixels and pure superpixels exist in an image. Nevertheless, mixed superpixels have negative effects on classification accuracy. Thus, it is necessary to generate superpixels containing as few mixed superpixels as possible for image classification. In this paper, first, a novel superpixels concept, named fuzzy-superpixels, is proposed for reducing the generation of mixed superpixels. In fuzzy-superpixels, not all pixels are assigned to a corresponding superpixel. We would rather ignore the pixels than assign them to improper superpixels. Second, a new algorithm is proposed to generate fuzzy-superpixels for PolSAR image classification. Three PolSAR images are used to verify the effect of the proposed fuzzy superpixels algorithm. Experimental results demonstrate the superiority of the proposed fuzzy-superpixels algorithm over several state-of-the-art superpixels algorithms.**

***Index Terms*—superpixels, fuzzy-superpixels, polarimetric synthetic aperture radar (PolSAR), image classification**

## I. Introduction

Image segmentation is a one of fundamental techniques in compute vision [1]. Many image segmentation algorithms have been proposed in the past few years [2], [3]. Superpixels method is a kind of image segmentation technique, which are usually used as a pre-processing step for computer vision applications. Superpixels are small image regions with homogenous appearance, which are generated by the over-segmentation of the original image. Superpixels-based operation has some advantages over pixels-based operation. First, superpixels preserve the structure information in images. Second, the computationally efficient can be improved by substituting thousands of pixels with a few hundreds of superpixels. Therefore, many computer vision applications benefit from working with superpixels instead of just pixels [4], [5].

In general, the good superpixels algorithms are capable to improve the performance of computer vision applications [6]. However, each superpixels algorithm has its own merits [7]. A more suitable superpixels algorithm should be selected for a specific application. For example, if superpixels are used to build a graph, Ncut algorithm [8] may be an ideal choice, which generates more regular superpixels with visually pleasing. If the running speed of algorithm is of paramount importance, SEEDS algorithm [4] may be a better choice. If superpixels are used as a pre-processing step in segmentation algorithms, a method that greatly improve the performance of the segmentation algorithms, such as SLIC [7], is probably a good choice.

Polarimetric synthetic aperture radar (PolSAR) image classification is one of the representative computer vision applications [9], [10]. PolSAR is capable of providing remotely sensed image information under dayor-night and all-weather conditions, which contains more available information than single polarization SAR as electromagnetic waves are transmitted and received in various polarimetric states [11]. As pixels-based classification techniques [12]–[15] only label each pixel independently and ignore the influence of the spatial relationship between pixels, speckle noise caused by coherent imaging mechanism seriously influence the classification performance of PolSAR image. Thus, superpixels-based PolSAR classification methods have been attracted widely attention [16]–[21].

The main steps of superpixels-based PolSAR image classification consist of superpixels generation, polarization features selection, sample selection and classification. The first step, superpixels generation, is commonly regarded as a pre-processing step in classification. Table I shows the pre-processing algorithms used in [16]–[21]. Superpixels has a significant impact on the performance of image classification. However, there is no specifically designed superpixels algorithm for image classification. In classification, all pixels in a superpixel are regarded as having the same labels. However, it is believed that both mixed superpixels and pure superpixels exist in practice applications [22]. In Fig. 1, different color blocks represent pixels with different labels. Suppose there are six superpixels in the image. Mixed superpixels consist

This work was supported by Project supported the Foundation for Innovative Research Groups of the National Natural Science Foundation of China, No.61621005, the National Natural Science Foundation of China, No.U1701267, No.61573267, No.61771379, No.61772400, No.61772401, No.61671350, No.61473215, No.61571342, No.61501353, No.61502369 and No.61701361, The Fund for Foreign Scholars in University Research and Teaching Programs (the 111 Project), No. B07048, the Major Research Plan of the National Natural Science Foundation of China, No. 91438201 and No. 91438103, the Program for Cheung Kong Scholars and Innovative Research Team in University, No. IRT_15R53.

Yuwei Guo, Licheng Jiao, Shuang Wang, Fang Liu and Wenqiang Hua are with the Key Laboratory of Intelligent Perception and Image Understanding of Ministry of Education, International Research Center for Intelligent Perception and Computation, Joint International Research Laboratory of Intelligent Perception and Computation, School of Artificial Intelligence, Xidian University, Xi'an, Shaanxi Province 710071, China. (e-mail: yuweiguo18@126.com)

Shuo Wang is with the Centre of Excellence for Research in Computational Intelligence and Applications (CERCIA), School of Computer Science, University of Birmingham, UK (e-mail: s.wang@cs.bham.ac.uk)

TABLE I
PRE-PROCESSING ALGORITHM USED IN POLSAR IMAGE CLASSIFICATION.

| [16] | [17] | [18] | [19] | [20] | [21] |
|---|---|---|---|---|---|
| Watershed | Mean shift | Ncut | Ncut | Modified SLIC | Ncut |

of pixels with various labels, such as the superpixels 2, 5, 6 in Fig. 1. Pure superpixels are composed of pixels from a single class, such as the superpixels 1, 3, 4. Given a labeled pixel, if the pixel is in a pure superpixel (e.g. pixel with symbol L in superpixels 1 of Fig. 1), then all the pixels in the pure superpixel are assigned to correctly label. However, if the pixel is in a mixed superpixel (e.g. pixel with symbol L in superpixels 5 of Fig. 1), then some pixels in the mixed superpixels are given a wrong label (e.g. only two pixels in superpixels 5 are given correct label, 14 other pixels are assigned a wrong label). Therefore, it is very important to design a specific superpixels algorithm for image classification application. The superpixels algorithm are urged to generate less mixed superpixels (or more pure superpixels) for reducing the negative effect of pre-processing step on classification performance.

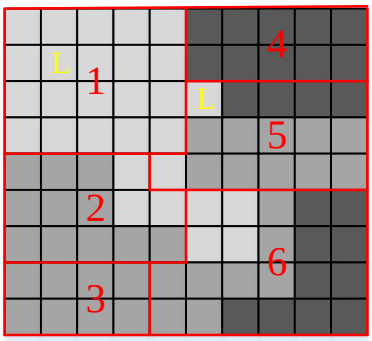


Fig. 1. An image with six superpixels.

For the above reasons, first, a novel superpixels concept, named fuzzy-superpixels, is specifically proposed for image classification application. The definition of fuzzy supepixels is based on enforcing producing less mixed superpixels. Pixels in an image are divided into two parts according to fuzzy-superpixels, superpixels and undetermined pixels. That is, not all pixels are assigned to a specific superpixel. Based on the concept of fuzzy-superpixels, we would rather ignore the pixels than assign them to an improper superpixel. Second, an algorithm, named FS, is presented to generate fuzzy-superpixels for PolSAR images classification. The main advantages of the proposed FS algorithm are as follows.
(1) FS is easy to be understood and realized.
(2) Boundary adherence of superpixels generated by FS is superior to which generated by the state-of-the-art superpixels algorithms. And FS yields more pure superpixels than other superpixels algorithms.
(3) FS is shown to outperform the existing superpixels algorithms when used for classification on PolSAR images.

The remainder of this paper is organized as follows. In Section II, the classical and the state-of-the-art superpixel generation algorithms are briefly reviewed. The concept of fuzzy-superpixels and the proposed superpixels algorithm FS are described in Section III. Section IV describes experiments and results. Conclusions and future works are given in Section V.

## II. RELATED WORK

In this section, we review modern superpixels generation techniques. Some algorithms are not originally designed specifically to generate superpixels, however, they would be introduced when reviewing algorithms for generating superixels [7].

**WS.** The watersheds-based algorithm is introduced by Luc Vincent in 1991 [23], which is a gradient-ascent-based method. The WS algorithm bases on immersion process analogy, and a queue of pixels is used to simulate the flooding of the water. The algorithm consists of two steps. In the first step, distributive algorithm is used to sort the gray value of pixels by ascending counts. The progressive flooding of the catchment basins of the image is executed in the second step. The watersheds-based algorithm often generates highly irregular superpixels, and the number of superpixels is not specified.

**Ncut.** Jianbo Shi et al. [8] propose a global criterion, the normalized cut, for segmenting the graph. Although Ncut is not originally designed to generate superpixels, it is usually used to produce superpixels [21], [24]. The normalized cut criterion minimizes the disassociation between the groups and maximizes the association within the groups. The generated superpixels by Ncut are very regular and have a good visual effect. However, the running speed of Ncut algorithm is slow for large images.

**MS.** Mean shift [25] is proposed for analyzing the feature space, which can be used to generate superpixels. MS is a popular non-parametric clustering algorithm, which bases on gradient ascent. Mode is defined as the center of a cluster, which is the local maximum of a probability density function. An iterative search strategy is used to find the modes of an image. As the step size in the iterative mode-seeking procedure is adaptive adjustment, it is easy to converge to local extremum points. Pixels in the basin of attraction of a mode are regarded as a superpixel. The structure of superpixels generated by MS is arbitrary. MS not offers direct control over the number of superpixels.

**QS.** In [26], another mode-seeking based superpixels generation algorithm, quick shift, is proposed by Andrea Vedaldi and Stefano Soatto. Quick shift is a simple and extremely efficient algorithm, which is introduced to address the over-fragmentation problem in medoid shift. In QS, each point in the feature space is moved to the nearest neighbor for an increment of the Parzen density function. Generated superpixels by QS have relatively good boundary adherence. And the number of superpixels does not need to be specified in advance.

**TP.** TurboPixels [27] bases on geometric flows to generate superpixels. Both local image boundaries and the limitation of the under-segmentation are considered in TP algorithm. The image is segmented by TP algorithm into a lattice-like structure of compact regions. That is, the generated superpixels

have approximately uniform size and shape. Authors claim that TP is a time-effective superpixels generation algorithm. However, for texture images, different objects are contained in the generated superpixels, and the weak boundary adherence is relatively poor.

**SLIC.** Radhakrishna Achanta et al. propose a simple linear iterative clustering algorithm to generate superpixels [7]. An adaptation of k-means clustering algorithm is used in SLIC. There are three steps in the algorithm. First, the cluster centers are initialized by sampling pixels on regular grids. Second, local k-means clustering is executed to assign every pixel to a single superpixel. At last, the disjoint segments are relabeled with the labels of the largest neighboring cluster for the connectivity of regions. The superpixels generated by SLIC have a good boundary adherence. The only parameter of SLIC algorithm is the desired number of superpixels.

**SEEDS.** The SEEDS algorithm is proposed in [4], which based on a simple hill-climbing optimization. The generation of superpixels is thought of as an energy maximization problem, which based on enforcing the color similarity within superpixels. Given an initial segmentation, superpixels are continuously refined by modifying the boundaries. The resulting superpixels have less regular size and shape. One of the main advantage of SEEDS is to run successfully in real time.

Superpixels generation algorithms have a same characteristic: each pixel is assigned to a specific superpixel.

## III. Fuzzy-superpixels based PolSAR image classification

First, with the consideration of the consistency of pixel label in a superpixel, the concept of fuzzy-superpixels is proposed. Instead of assigning each pixel to a relevant superpixel, fuzzy-superpixels allow a part of undetermined pixels. Second, an algorithm is proposed to generate fuzzy-superpixels. At last, a simple supervised classification process is designed.

### A. Concept of Fuzzy-superpixels

The superpixels generated by algorithms mentioned in Section II can be defined as traditional superpixels. Each pixel is assigned to a superpixel, and all pixels in each superpixel are regarded as having the same label. Fig. 2 shows an example of traditional superpixels. Suppose an image consists of 81 pixels, and each pixel is represented by a circle. The image is divided into six superpixels, and each superpixel is represented by a color. The performance of superpixels based classification algorithms depends on the generated superpixels. If the generated superpixel is not pure superpixel, i.e., pixels in a superpixel do not have a same label, the classification accuracy of pixels in the superpixel can never reach 100 percent no matter how wonderful classification algorithms are used. The classification performance is influenced seriously by the consistency of pixel label in a superpixel.

In order to increase the consistency of pixel label in a superpixel and generate more pure superpixels, a novel superpixels concept, fuzzy-superpixels, is proposed. In fuzzy-superpixels, not all pixels are assigned to a certain superpixel. If a pixel cannot be explicitly identified to a superpixel, the pixel is regarded as an undetermined pixel and not belongs to any superpixels. Fuzzy-superpixels are composed of two parts, the superpixels and the undetermined pixels. The example of fuzzy-superpixels is shown in Fig. 3. Suppose the image is $9 \times 9$ in size. Pixels in the image are represented with 7 different colors. Besides white, other kinds of colors represent different superpixels. The pixels shown by white circle are undetermined pixels. Compared with the result of superpixel algorithms (the dotted lines), there are some spacing between superpixels generated by fuzzy-superpixels. In summary, according to the concept of fuzzy-superpixels, pixels in an image are divided into two parts, superpixels and undetermined pixels. Pixels in the superpixels are regarded as a whole and are assigned to a same label. The labels of the undetermined pixels are needed to be assigned in the future process.

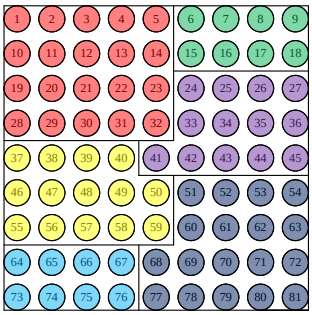

Fig. 2. The example of traditional superpixels

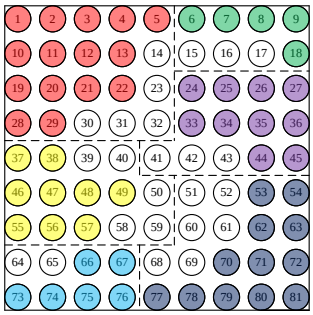

Fig. 3. The example of fuzzy-superpixels

### B. Generation of Fuzzy-superpixels

A new superpixels generation algorithm, named FS, is proposed to generate fuzzy-superpixels for PolSAR image. FS algorithm clusters pixels according to pixel location and the property of PolSAR images. FS algorithm is done in the 3-$D$ $[Cov, X, Y]$ space, where $Cov$ is the polarimetric covariance matrix of the pixels and $X, Y$ is the position of the pixels. There are four steps to generate fuzzy-superpixels by FS. First, the cluster centers are initialized. Second, identify overlapping and non-overlapping search regions. Third, generate fuzzy-superpixels, i.e., pixels are divided into two parts, superpixels and undetermined pixels. At last, the post-processing step.

Suppose $N$ is the number of pixels in an image, and $K$ is the expected number of superpixels. The size of the expected superpixels is less than $S = \sqrt{N/K}$. The initialization of cluster centers in FS just like it does in [7]. The initial cluster centers are selected on a regular grid spaced $S$ pixels apart, and the grid interval is set to $S$. In order to avoid the cluster center falling on an edge or a noisy pixel, the cluster centers are moved to the lowest gradient position in a $3 \times 3$ neighborhood. Instead of searching all pixels for a cluster center, the size of the search region is reduced to $2S \times 2S$ for speeding up FS algorithm.

FS algorithm adapts fuzzy c-means (FCM) [28] clustering algorithm to generate superpixels. According to the initial clustering centers and the given search regions, the overlapping

and non-overlapping research regions are identified. Pixels in the non-overlapping regions belong to the corresponding superpixel. Pixels in the overlapping regions are measured as follows.

The degree of membership between pixels in overlapping region and the center pixels corresponding to the overlapping region are estimated by optimizing the object function.

For any pixel, the sum of the degree of membership is 1, which is defined as follow:

$$\sum_{i=1}^{n} u\left(i,j\right)=1, \forall j=1,...,c \tag{1}$$

where, $i$ is the pixel in the overlapping search regions. $j$ is the corresponding center pixels. $c$ is the total number of the center pixels corresponding to the pixel $i$.

A generalized form of the objective function is shown:

$$J\left(U,C_1,...,C_c\right)=\sum_{j=1}^{c}J_j=\sum_{j=1}^{c}\sum_{i=1}^{n}u^m\left(i,j\right)D_{polsar}^2\left(i,j\right) \tag{2}$$

where, $u\left(i,j\right)\in[0,1]$, $C_1,...,C_c$ is the center pixels, $m\in[1,\infty)$ is a weight index, and $D_{polsar}$ is a distance measure between the pixel $i$ and the center pixel $j$.

The distance measure $D_{polsar}$ in FS is a revised version of the distance measure used in [7]. Both PolSAR image property and position proximity are taken into consideration in $D_{polsar}$. The revised distance measure applies to PolSAR image processing, which is defined as follows [29].

$$D_{polsar}\left(i,j\right)=\sqrt{\left(\frac{d_w\left(i,j\right)}{mpol}\right)^2+\left(\frac{d_{xy}\left(i,j\right)}{S}\right)^2} \tag{3}$$

where, $d_w\left(i,j\right)$ and $d_{xy}\left(i,j\right)$ denote Wishart distribution-based distance and position proximity, respectively. $mpol$ is a parameter to balance the importance of wishart distribution-based distance and position proximity. The larger the value $mpol$, the more important the position proximity.

$$d_w\left(i,j\right)=\ln\left(\left|\Sigma_j\right|\right)+\mathrm{Tr}\left(\Sigma_j^{-1}\mathrm{T}_i\right) \tag{4}$$

$$d_{xy}\left(i,j\right)=\sqrt{\left(x_j-x_i\right)^2+\left(y_j-y_i\right)^2} \tag{5}$$

$d_w\left(i,j\right)$ is Wishart distribution-based distance [30], which is a statistical model-based measure and is more suitable than Euclidean distance for PolSAR image. $\Sigma_j$ is the mean coherency matrix of the superpixel centered at $j$, and $\mathrm{T}_i$ is the coherency matrix of pixel $i$. Covariance matrix $Cov_i$ can convert to coherency matrix $\mathrm{T}_i$. $\mathrm{T}_i=VCov_iV^{-1}$, and $V=\frac{1}{\sqrt{2}}\begin{bmatrix}1&0&1\\1&0&-1\\0&\sqrt{2}&0\end{bmatrix}$.

The new objective function is constructed for computing the necessary condition to make $J\left(U,C_1,...,C_c\right)$ to a minimum. The revised objective function is shown:

$$\begin{aligned}&\overline{J}\left(U,C_1,...,C_c,\lambda_1,...,\lambda_n\right)\\&=J\left(U,C_1,...,C_c\right)+\sum_{i=1}^{n}\lambda_i\left(\sum_{j=1}^{c}u\left(i,j\right)-1\right)\\&=\sum_{j=1}^{c}\sum_{i=1}^{n}u^m\left(i,j\right)D_{polsar}^2\left(i,j\right)\\&\quad+\sum_{i=1}^{n}\lambda_i\left(\sum_{j=1}^{c}u\left(i,j\right)-1\right)\end{aligned} \tag{6}$$

where, $\lambda_i, i=1,...,n$ is lagrangian multiplier.

The necessary condition of minimizing $\overline{J}\left(U,C_1,...,C_c,\lambda_1,...,\lambda_n\right)$ is computed through taking the derivative of $\overline{J}\left(U,C_1,...,C_c,\lambda_1,...,\lambda_n\right)$, and the necessary condition is shown:

$$c_j=\frac{\sum_{i=1}^{n}u^m\left(i,j\right)x_i}{\sum_{i=1}^{n}u^m\left(i,j\right)} \tag{7}$$

$$u\left(i,j\right)=\frac{1}{\sum_{k=1}^{c}\left(\frac{D_{polsar}(i,j)}{D_{polsar}(i,k)}\right)^{2/(m-1)}} \tag{8}$$

The center pixels and the degree of membership of pixels in overlapping search regions are obtained through Eq. 7 and Eq. 8. The degree of membership of pixel is used to determine whether a pixel belongs to a superpixel. The process is described as follows.

Suppose $U=[U_1,...,U_i,...,U_n]$, $U_i=[u_{i1},...,u_{ij},...,u_{ic}]$ is the membership degree of pixel $i$ to center pixels $[C_1,...,C_c]$. The maximum value in $U_i$ is defined as $U_{i\max}$, and $U_{\max}=[U_{1\max},...,U_{i\max},...,U_{n\max}]$. The center pixel corresponding to the maximum value is defined as $P_{\max}=[P_{1j},...,P_{ij},...,P_{nj}]$, $j\in 1,...,c$. The sub-maximum value vector of U is depicted by $U_{sub\max}=[U_{1sub\max},...,U_{isub\max},...,U_{nsub\max}]$.

$$\begin{aligned}Udiff&=U_{\max}-U_{sub\max}\\&=[Udiff_1,...,Udiff_i,...,Udiff_n]\end{aligned} \tag{9}$$

$$UdiffMed=median\left(Udiff\right) \tag{10}$$

where, $median\left(\bullet\right)$ computes the intermediate value of vector $\bullet$.

$\forall i\in n$, if $Udiff_i>UdiffMed$, then pixel $i$ belongs to the superpixel with center pixel $P_{ij}$. Otherwise, $i$ is an undetermined pixel.

The fuzzy clustering result is often broken, which is due to FS algorithm does not explicitly enforce connectivity. Like other superpixels algorithm [7], [29], a post-processing step is used to enforce region connectivity. Our post-processing strategy is straightforward.

For each undetermined pixel $up$, suppose the size of the search region centering $up$ is $M\times M$. In the region, the number of superpixels $Num_s$ is computed. If $Num_s>1$, the pixels in the region are assigned to undetermined pixels. If $Num_s=1$, the pixels in the region are assigned to the superpixels. In our experiments, the size of the search region is set to $7\times 7$.

**Algorithm 1:** FS

**Input:** $K, m, mpol, epsilon, itmax$

**Output:** fuzzy-superpixels

Step1: Initialization of the cluster centers $Cen_i = [Cov_i, x_i, y_i]^T$, $i = 1, ..., k$ by sampling pixels at regular grid.
Step2: Move cluster centers to the lowest gradient position in a $3 \times 3$ neighborhood.
Step3: Identify the overlapping search region set $OverlapRegion$.
Step4: For each region $r$ in $OverlapRegion$
Step5: $stable = 0$;
Step6: while $it < itmax \&\& stable = 0$
Step7: According to Eq. 3, compute the distance $D_{polsar\_r}$ between the pixles in region $r$ and cluster centers $OverCen_r$ corresponding to the region $r$.
Step8: Update matrix $U_r$ according to Eq. 8.
Step9: Compute the cluster centers according to Eq. 7.
Step10: $Cen = OverCen_r - C_r$.
Step11: Compute the Frobenius norm $fnorm$ of $Cen$
Step12: if $fnorm < epsilon$
Step13: $stable = 1$;
Step14: end
Step15: it = it + 1;
Step16: end
Step17: end
Step18: $Udiff = U_{\max} - U_{sub\max}$.
Step19: $UdiffMed = median\,(Udiff)$.
Step20: if $Udiff < UdiffMed$
Step21: the pixels are undetermined pixels;
Step22: else
Step23: the pixels are assigned to the corresponding superpixels;
Step24: end
Step25: The pixels in the non-overlapping regions belong to the corresponding superpixel.
Step26: The post-processing.

The FS algorithm is summarized in Algorithm 1.

In order to better understand the FS algorithm, an example is given to explain the generation of fuzzy superpixels. There are 81 pixels in an image, which is shown in Fig. 4. Suppose the center pixels are selected, and the corresponding search regions size is $5 \times 5$. The initial fuzzy-superpixels center pixels are 8, 21, 34, 48, 61 and 75, which correspond to 6 expected fuzzy superpixels regions and are represented by 6 different colors. The search regions of different center pixels are differentiated with the different color rectangle. For example, the red rectangle is the search region of the center pixel 21. From Fig. 4 we can see that the search regions include non-overlapping regions and overlapping regions. The pixels in non-overlapping search regions are assigned to the corresponding superpixel. For instance, pixel 1 is in the non-overlapping search region of the center pixel 21, that is, the search regions of other center pixels do not contain the pixel 1. Therefore, the pixel 1 belongs to the superpixel with center pixel 21. Besides non-overlapping regions, there are some overlapping regions. The pixels in the overlapping regions are labeled with mixed colors, which are shown in Fig. 5. For instance, the pixel 41 is in the overlapping search regions of center 21, 34, 48 and 61, which is labeled with 4 different colors. It is easy to see that pixel 41 may belong to the superpixel with center pixel 21, with center pixel 34, with center pixel 48 or with center pixel 61. In fuzzy superpixels, pixel 41 cannot be grouped into any superpixel if conditions are not meet, then pixel 41 is an undetermined pixel.

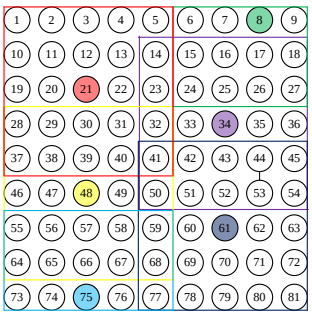

Fig. 4. The search regions.

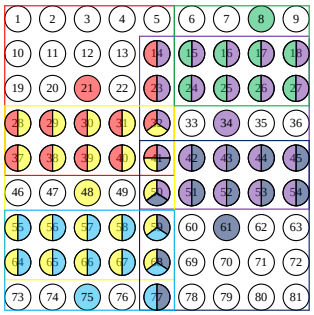

Fig. 5. The pixels in the search regions

In summary, FS is a four-step process and the main procedure of FS is as follows.
(1) Initialize the cluster centers of fuzzy superpixels and set the expected number of fuzzy superpixels.
(2) Find out non-overlapping search regions and overlapping search regions according to the number of fuzzy superpixels and the cluster centers.
(3) For the pixels in the overlapping search region, the membership degree between the pixel and center pixels are computed. And the membership degree is used to estimate whether a pixel belongs to a superpixel. The pixels in the non-overlapping search region are assigned to the corresponding superpixels.
(4) The post-processing step.

## IV. Experimental Results and Analysis

In order to evaluate the effectiveness of the proposed FS algorithm, we present and analyse the experimental results by applying the proposed FS algorithm on three PolSAR images. The proposed algorithm are compared with the classical and the state-of-the-art superpixel algorithms. Furthermore, the performance of classification resulting from superpixels and fuzzy-superpixels are analyzed.

### A. Description of Experimental Data Sets

*Flevoland.* The first data set is a subset of an L-Band multilook PolSAR image, acquired by the AIRSAR airborne platform in 1989. The scene covers the Flevoland, Netherlands. The false color image obtained by Pauli decomposition is shown in Fig. 6(a), the size of which is $300 \times 270$. The ground truth map is obtained by referencing [31], and it is shown in Fig. 6(b). Fig. 6(c) is the color code representing different classes. According to the ground truth map, pixels in

the region are classified into six basic classes, i.e., bare soil, potatoes, beet, forest, wheat, and peas.

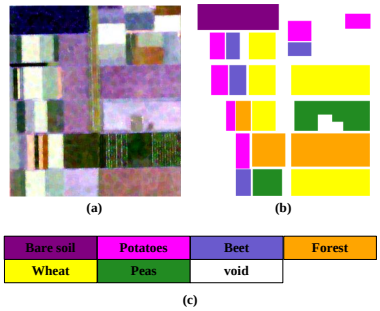


Fig. 6. Flevoland. (a) PolSAR image (PauliRGB). (b) The ground truth map. (c) Color code.

*ESAR*. The second data set is obtained from an L-band multilook PolSAR image, which is provided by the German Aerospace Center's E-SAR. The scene covers Oberpfaffenhofen, Germany. The experimental image is shown in Fig. 7(a), the size of which is 1300 $\times$ 1200. The ground truth map is obtained by referencing [19], and it is shown in Fig. 7(b). The color code of ground truth map is shown in Fig. 7(c). According to the ground truth map, there are three classes in the second data set: Built-up areas, wood land and open areas.

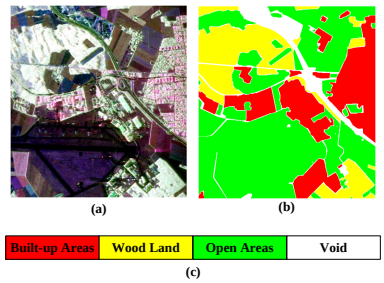


Fig. 7. Esar. (a) PolSAR image (PauliRGB). (b) The ground truth map. (c) Color code.

*San Francisco*. The third data set is the area around the bay of San Francisco with the golden gate bridge, which is one of the most used data set in PolSAR image classification in the past years. A good coverage of both natural targets and man-made targets is provided by San data set. The size of the used image is 1300 $\times$ 1300, and the Pauli RGB image is shown in Fig. 8(a). The ground truth map is obtained by referencing [32], which is shown in Fig. 8(b). The data set mainly contains five terrain classes, which are low-density urban, water, vegetation, high-density urban and developed. The corresponding color code is shown in Fig. 8.

For the three PolSAR data set, each class indicates a type of land covering and is identified by one color. It is noting that pixels without ground truth are categorized as void.

### B. Parameter Analysis

Two parameters $mpol$ and $K$ are required in FS algorithm, which offer control over superpixels compactness and the desired number of superpixels, respectively. Pure superpixels ratio (PSR) is used as the evaluation measure to evaluate the

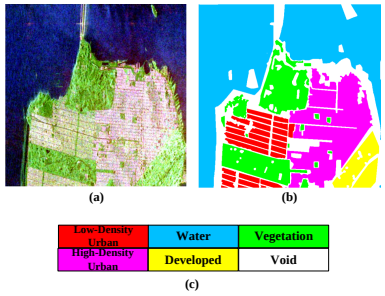


Fig. 8. SanFrancisco. (a) PolSAR image (PauliRGB). (b) The ground truth map. (c) Color code.

influence of the two parameters. Suppose the number of pure superpixels is $\mathrm{Num}_p$, and the number of superpixels with labeled pixels is $\mathrm{Num}_L$. PSR is defined as $\mathrm{Num}_p/\mathrm{Num}_L$.

The first experiment is to investigate the impact of the parameter $mpol$. Suppose the amount of superpixels is set to 500 for Flevoland, ESAR and San Francisco. The parameter $mpol$ is set from 1 to 60 with an interval of 5. The impact is assessed by comparing the pure superpixels ratio of FS with different parameter $mpol$. The curve of the pure superpixels ratio on three datasets are shown in Fig. 9. The x-axis is $mpol$, and the y-axis is the pure superpixels ratio. From these curves we can see that a relatively high pure superpixels ratio can be obtained when $mpol$ in a range from 20 to 25 for Flevoland, from 35 to 55 for Esar, and from 45 to 55 for San Francisco. Therefore, in the following experiments we set the parameter $mpol$ to 20, 50, and 50 for Flevoland, Esar and San Francisco, respectively.

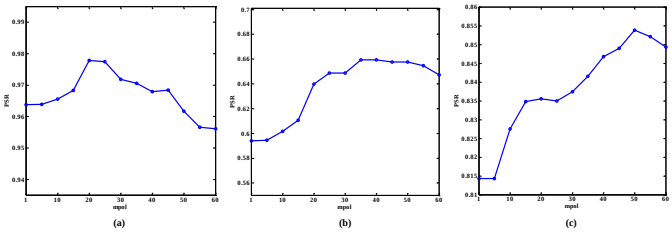


Fig. 9. Parameter $mpol$. (a) Flevoland. (b) Esar. (c) San Francisco.

To evaluate the effect of the number of generated superpixel on pure superpixels ratio, the number of generated superpixels is set in a range from 100 to 500 for Flevoland. For Esar and San Francisco, the number of generated superpixels ranges from 500 to 3000. It is note that the number of superpixels generated by various superpixel algorithms is approximately the same with the set value. This is widely admitted in superpixel algorithms [7], [27]. For the three data set, the pure superpixels ratios under various amount of superpixels are shown in Fig. 10, from which we can see that the pure superpixels ratio increased with the number of generated superpixels increasing.

### C. Performance of Fuzzy Superpixels

In this section, we compare FS with six superpixel algorithms. These algorithms include Mean Shift(MS) [25],

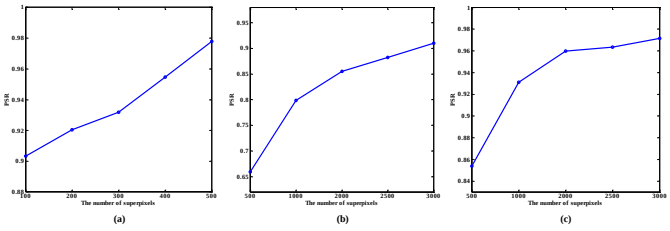


Fig. 10. Parameter $K$. (a) Flevoland. (b) Esar. (c) San Francisco.

Quick Shift(QS) [26], Normalized cuts(Ncut) [8], TurboPixels(TP) [27], SLIC [7] and SEEDS [4]. For all six algorithms, the implementations are based on publicly available codes. MS algorithm is implemented by employing the Edge Detection and Image Segmentation (EDISON) System [1]. The system was developed by the Robust Image Understanding Laboratory at Rutgers University, which contains mean shift based image segmentation algorithm. QS and SLIC are implemented by using the VLFeat open source library [2]. VLFeat is written in C for efficiency and compatibility, with interfaces in MATLAB for ease of use. The source codes of Ncut, TP and SEEDS are provided by their authors' web pages [3] [4] [5]. The smoothness parameter in Ncut is set to 0.005, 0.05 and 0.07 for Flevoland, Esar and San Francisco, respectively, which we find to have the highest pure superpixels ratio. For Flevoland data set, the number of generated superpixels is set from 200 to 500. For ESAR and San Francisco data set, the range of the number of generated superpixels is from 500 to 3000. In addition to evaluation measure PSR, two commonly used evaluation measures are adopted to measure the performance of superpixels algorithms. They are the under segmentation error (UE) and the boundary recall (BR). For UE, the lower the better, and for BR and PSR, the higher the better.

*1) Under-Segmentation Error (UE):* A superpixel should only overlap one object. The deducting area is defined as the superpixels that overlaps the ground-truth segmentation result. The UE is computed by averaging the deducting area over all the ground truth segmentations, which is defined as follows:

$$UE = \frac{1}{\sum_{j=1}^{L}|s_j|}\left(\sum_{i=1}^{M}\sum_{s_j|s_j\cap g_i>0}|s_j| - \sum_{j=1}^{L}|s_j|\right) \qquad (11)$$

where $s_j$ are the superpixels generated by algorithm, and the total number of superpixels is $L$. $g_i$ are the ground truth segmentation result, and the number of segmentation is $M$. $|s_j|$ indicates the number of pixels in superpixels $s_j$. It is note that only superpixels part is considered in computing the UE of fuzzy superpixels. Fig. 11 gives the UE of superpixel results produce by MS, QS, Ncut, TP, SLIC, SEEDS and FS on the three PolSAR images. From Fig. 11 we can see that our algorithm FS achieves lower value than the other six algorithms. A lower UE indicates that fewer superpixels contains multiple objects.

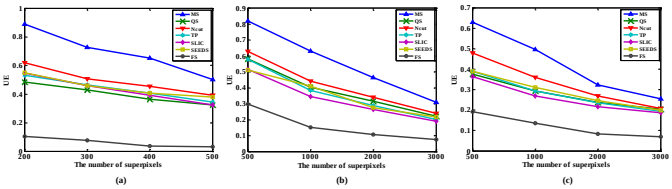


Fig. 11. UE. (a) Flevoland. (b) Esar. (c) San Francisco.

*2) Boundary Recall (BR):* The BR measures the performance of superpixels by considering the boundary adherence. The BR is defined as the ratio of the ground truth boundaries that fall within the nearest superpixel boundaries. Like in [4], a standard measure of BR is used, which is defined as follows:

$$BR = \frac{1}{PN}\left(\sum_{p=1}^{P} N\text{logical}(\min_{y_q}\|x_p - y_q\| < 2)\right) \qquad (12)$$

where $x$ and $y$ are the boundary pixels obtained from the ground truth and the superpixel results, respectively. $PN$ denotes the number of pixels in the boundary of ground truth result. Fig. 12 shows that in most case FS achieves highest BR value than other superpixels algorithms. A higher BR indicates that fewer true boundaries are missed.

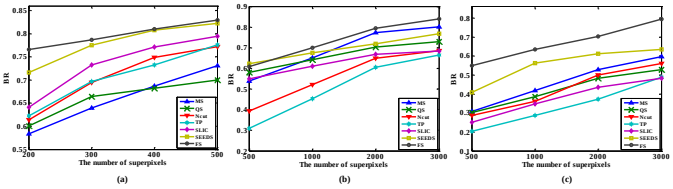


Fig. 12. BR. (a) Flevoland. (b) Esar. (c) San Francisco.

*3) Pure Superpixels Ratio (PSR):* The PSR measures the ability of superpixels algorithms to produce pure superpixels. Fig. 13 presents the PSR for the three dataset. From Fig. 13 we can see that FS algorithm can generate more pure superpixels than other superpixel algorithms.

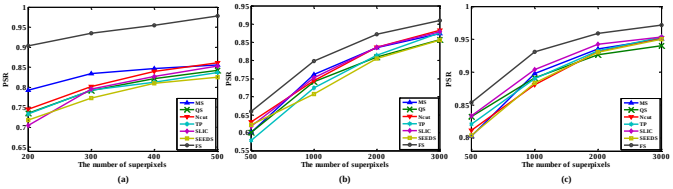


Fig. 13. PSR. (a) Flevoland. (b) Esar. (c) San Francisco.

*4) Superpixels visual display:* Fig. 14 and Fig. 16 show the superpixel results using Flevoland ground truth map with 200 and 500 superpixels, respectively. Superpixels generated by FS algorithm are represented by enclosed areas with lines, and these areas do not connect with each other. Pixels not belonging to superpixels are undetermined pixels. In order to better observe the generated superpixels, one or two regions

[1] http://coewww.rutgers.edu/riul/research/code/EDISON/
[2] http://www.vlfeat.org/
[3] http://www.cis.upenn.edu/%7Ejshi/software/
[4] http://www.cs.toronto.edu/%7Ebabalex/research.html
[5] http://www.mvdblive.org/seeds/

are selected to enlarged, which are marked with blue rectangle. The enlarged regions are shown in Fig. 15 and Fig. 17. In Fig. 15, there are three colours representing three classes: potatoes, beet and wheat. Some potatoes and beet are divided into a superpixels by MS, QS, Ncut, TP, SLIC and SEEDS algorithm. Some beet and wheat are assigned to a superpixels according to QS, Ncut, TP and SLIC algorithms. Superpixels generated by FS adhere well to classes boundaries than other superpixels generation algorithms. The Fig. 17 presents the enlarged image of two regions in Fig. 16.

Superpixels on the ground truth map of Esar are shown in Fig. 18, the number of superpixels in which are 1000. In Fig. 18, two regions are seleced to enlarged. The enlarged regions are represented in Fig. 19.

Superpixel results on SanFrancisco ground truth image with 500 superpixels are shown in Fig. 20. Two regions are marked with blue rectangle in the ground truth image with 500 superpixels. The enlarged images of the marked regions are shown in Fig. 21.

According to the visual comparison of superpixels generated by various algorithms, we can see that:
(1) The size of superpixels becomes smaller and the performance of boundary preserving are better by increasing the number of generated superpixels.
(2) Superpixels generated by MS, QS and SEEDS are irregular. FS produces relative regular and visually pleasing superpixels.
(3) Superpixels generated by FS more pure than those generated by other algorithms.

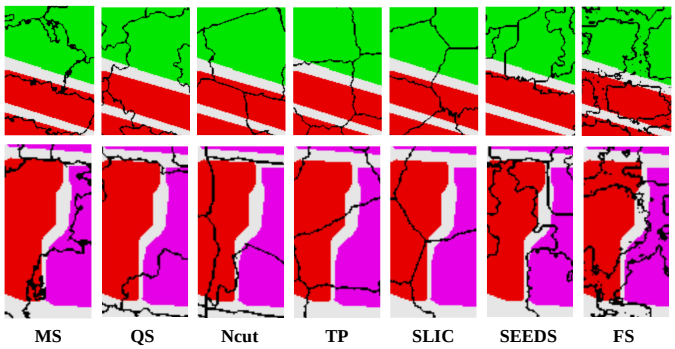


Fig. 21. SanFrancisco, the number of superpixels is 500. The enlarged images of the selected regions.

*5) Time complexity:* The time complexity of the traditional FCM algorithm is $O(cIN)$, where $c$ is the total number of the cluster centers, $I$ denotes the number of iterations, $N$ is the number of pixels in an image. FS is specifically designed to the superpixel clustering problem using a modified FCM. In FS, local search strategy is employed and only the pixels in overlapping search region are judged whether belong to a superpixel. The operations avoid performing thousands of redundant distance calculations. In addition, a pixel falls in the search regions of up to four cluster centers in practice. Thus, the proposed FS is $O(N)$ complex, the complexity of which is linear in the number of pixels in overlapping search region. The computational complexity of the various superpixels algorithms are shown in Table II.

### D. Superpixels-based classification performance

Superpixels algorithms are usually used as a preprocessing step. In superpixels-based classification algorithms, each superpixel is regarded as a processing element. In order to verify the effect of superpixels algorithms, a simple supervised classification process is used.

A pixel in PolSAR image can be represented by a coherency matrix $T$:

$$T = \begin{bmatrix} A & D - jE & F + jG \\ D + jE & B & H + jK \\ F - jG & H - jK & C \end{bmatrix} \tag{13}$$

Coherency matrix contains fully polarimetric information and the second-order statistics of polarimetric information. The PolSAR data in this paper is represented by the coherency matrix itself, without any manual feature extraction. A column vector is used to express a pixel in a PolSAR image: $I = [A, B, C, D, E, F, G, H, K]^T$, where superscript $T$ denotes a transposition. All pixels in a PolSAR image are represented as: $AllP = \{I_1, ..., I_i, ..., I_N\}$, where $I_i$ is the $i$th pixel, $N$ denotes the total number of pixels in the PolSAR image.

For each dataset, five labeled pixels are randomly selected from each class. Superpixels with labeled pixels are assigned to the same label with the corresponding labeled pixels. Each superpixel is represented by the mean value of pixels in the superpixel. Different from other superpixels algorithms, pixels in FS are divided into two parts, superpixels and undetermined pixels. For superpixels part, each superpixel is also represented by the mean value of pixels in the superpixel. For undetermined pixels part, each pixel is a processing element. The labeled superpixels are the training set, and the residual parts are the test set. SVM is used as classifier, because it is frequently applied to SAR classification problems [32]. Each experiment is performed 50 times on every data set. The average classification accuracy is recorded for comparison. The classification accuracy is the percentage of pixels belonging to each class that are categorized to the correct class. It is noting that the void pixels are ignored in computing the classification accuracy.

*1) Flevoland data set:* The classification accuracy of the proposed algorithm and seven comparing algorithms are shown in Table III. PB indicates that each pixel is regarded as a processing element in the classification experiments. In other algorithms, superpixel is the processing element. Superpixels are produced by MS, QS, Ncut, TP, SLIC, SEEDS and FS, respectively. The number of superpixels are 200 and 500, respectively. From Table III, we conclude that the superpixels-based classification outperform PB, since spatial relations between pixels are taken into consideration. FS has better classification accuracy, which is about 7.12%, 4.84%, 5.48%, 3.51%, 3.53% and 5.07% higher than other superpixel algorithms with 500 superpixels, respectively.

The total accuracy of each algorithm by repeatedly running 50 is demonstrated in Fig. 22. From the boxplot, we can see that compared with other algorithms, FS algorithm has better stability.

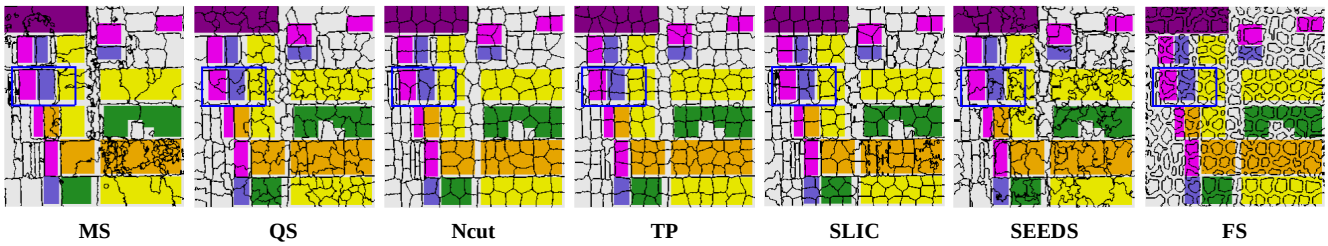


Fig. 14. Flevoland, the number of superpixels is 200.

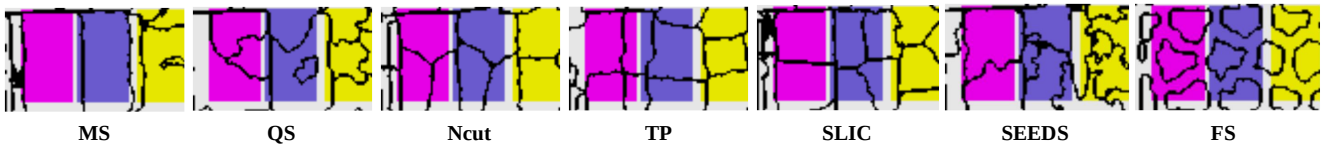


Fig. 15. Flevoland, the number of superpixels is 200. The enlarged images of the selected region.

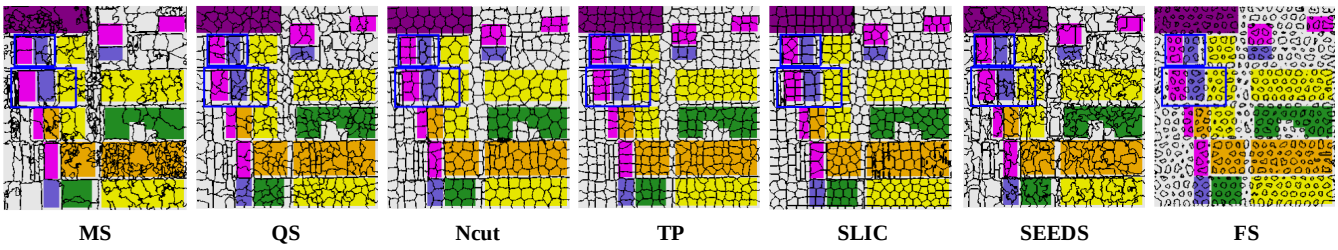


Fig. 16. Flevoland, the number of superpixels is 500.

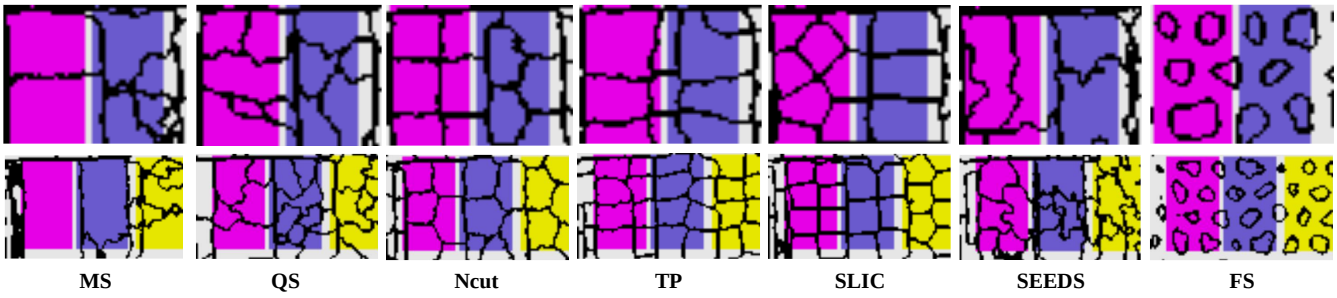


Fig. 17. Flevoland, the number of superpixels is 500. The enlarged images of the selected regions.

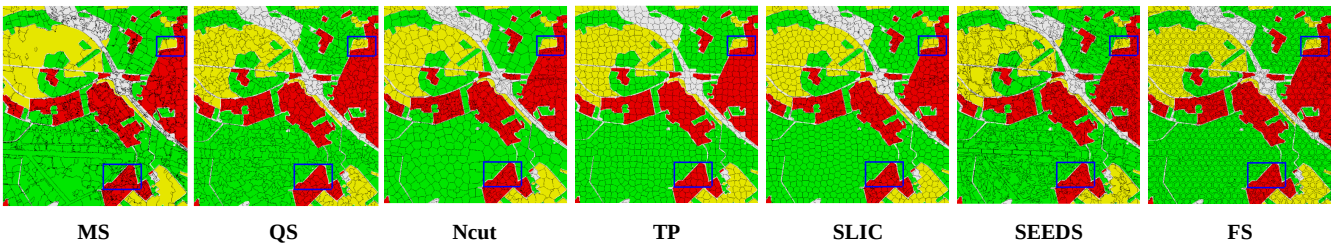


Fig. 18. Esar, the number of superpixels is 1000.

TABLE II
THE COMPUTATIONAL COMPLEXITY OF SUPERPIXELS ALGORITHMS.

| MS | QS | Ncut | TP | SLIC | SEEDS | FS |
|---|---|---|---|---|---|---|
| $O\left(N^2\right)$ | $O\left(dN^2\right)$ | $O\left(N^{\frac{3}{2}}\right)$ | $O\left(N\right)$ | $O\left(N\right)$ | $O\left(N\right)$ | $O\left(N\right)$ |

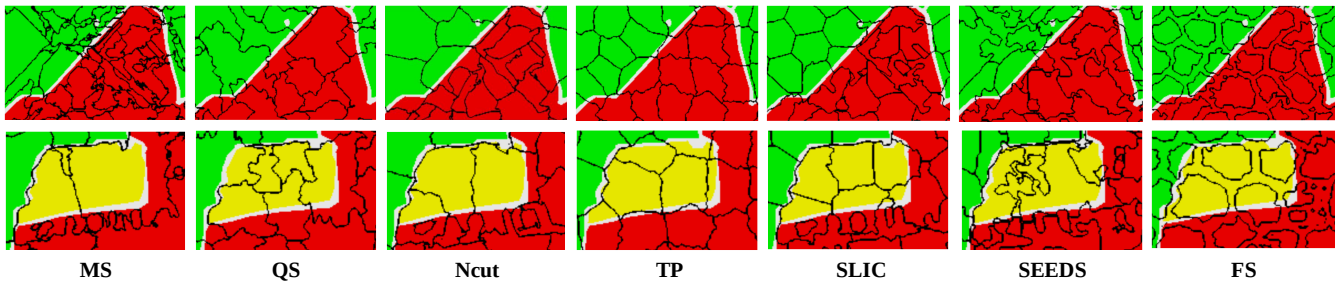


Fig. 19. Esar, the number of superpixels is 1000. The enlarged images of the selected regions.

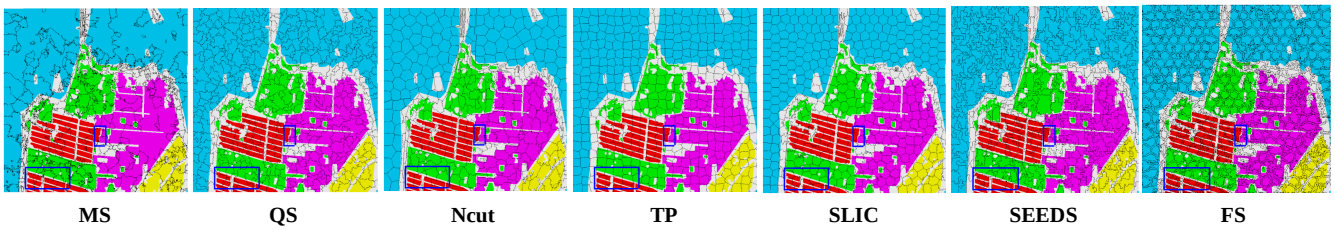


Fig. 20. SanFrancisco, the number of superpixels is 500.

TABLE III
FLEVOLAND. THE AVERAGE ACCURACY RATE AND STANDARD DEVIATION (STD) ACORSS 50 TESTS. THE BEST RESULT FOR EACH DATASET IS IN BOLD. (MEAN%±STD%)

| | PB | MS | QS | Ncut | TP | SLIC | SEEDS | FS |
|---|---|---|---|---|---|---|---|---|
| 200 | 70.77±6.9 | 80.79±5.6 | 79.48±9.4 | 81.70±6.9 | 83.66±5.9 | 80.95±5.9 | 83.31±5.0 | **86.70±3.2** |
| 500 | 70.77±6.9 | 80.23±6.5 | 82.51±5.2 | 81.87±6.1 | 83.84±5.1 | 83.82±5.3 | 82.28±5.2 | **87.35±1.9** |

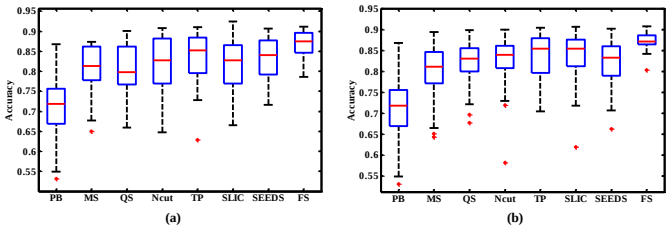


Fig. 22. Flevoland. (a) The number of superpixels is 200. (b) The number of superpixels is 500.

For Flevoland with 500 superpixels, the classification results overlaying on the ground-truth results are illustrated in Fig. 23. Black indicates the classification results are not same with the ground truth results. The enlarge images of the two selected regions marked with blue rectangle are shown in Fig. 24. From the visual effects of various superpixels-based classification results, we can see that: The result of PB is not well in regional continuity than superpixel-based algorithms. It is because pixels are regarded as processing elements in PB. Pixels-based classification algorithms are very sensitive to speckle noise. The classification results based on MS, QS, Ncut, TP, SLIC and SEEDS algorithms maintain the regional continuity. However, some large areas may be given a wrong label. Such as, MS Fig. 24(b), QS Fig. 24(b), Ncut Fig. 24(b), TP Fig. 24(b), SLIC Fig. 24 (a) and SEEDS Fig. 24 (b). FS-based classification algorithm balance between PB classification algorithm and superpixels-based classification algorithms. The result of FS-based algorithm have a better visual effect than PB and have less large incorrectly areas than other superpixels-based algorithms. It is confirmed the conclusion that FS does achieve better classification performance, compared with PB, MS, QS, Ncut, TP, SLIC and SEEDS.

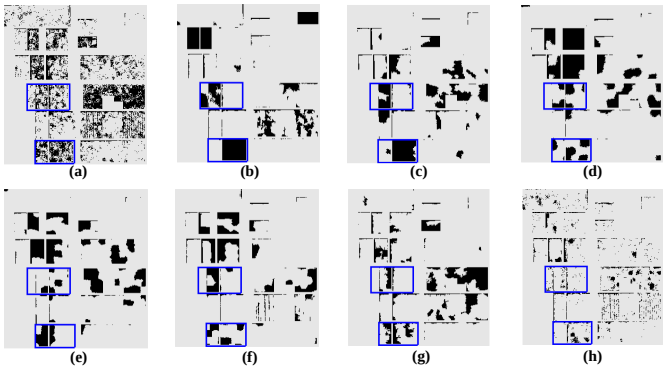


Fig. 23. Flevoland. The classification results with 500 superpixels. (a)-(h) are PB, MS, QS, Ncut, TP, SLIC, SEEDS and FS, respectively.

*2) ESAR data set:* Table IV lists the classification accuracy on Esar obtained by the aforementioned eight algorithms. The number of superpixels are 500, 1000 and 3000, respectively. From the experimental results in Tabel IV, we can see that: (1) When the number of generated superpixels is 500, superpixels-based classification results does not always better

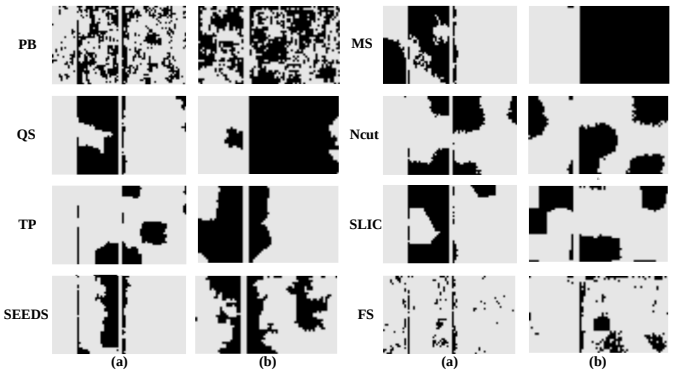


Fig. 24. Flevoland. The enlarged images of the selected regions.

than PB classification result. It is due to the poor superpixels results. If the number of superpixels is too small, it might give rise to under-segmentation in some areas.

(2) The average classification accuracy of FS on various number of superpixels is about 5.53%, 6.85%, 7.28%, 5.45%, 5.21%, 5.87% and 4.18% higher than other superpixel algorithms, respectively.

(3) The results on superpixels 1000 are better than the results on superpixels 3000. The reason is that: the more the number of generated superpixels, the smaller the size of superpixels. And small superpixels are more easily affected by speckle noise.

Boxplots are used to present the total accuracy with superpixels 500 and 1000, which is shown in Fig. 25.

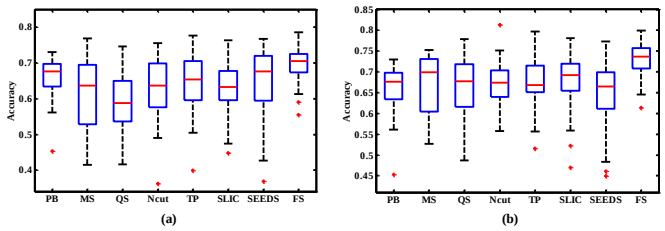


Fig. 25. Esar. (a) The number of superpixels is 500. (b) The number of superpixels is 1000.

Fig. 26 shows the classification results of Esar with 1000 superpixels. The enlarged images of the regions marked with blue rectangle are shown in Fig. 27. The visual comparison of classification result obtained by various algorithms shows that large amount of areas are misclassified by PB and superpixels-based algorithms. Such as, PB Fig. 27(a), MS Fig. 27(b), QS Fig. 27(a), Ncut Fig. 27(a), TP Fig. 27(a), SLIC Fig. 27(a) and SEEDS Fig. 27(a).

*3) San Francisco data set:* The classification accuracy on San Francisco computed by the eight algorithms are shown in Table V. The number of superpixels are 500, 1000 and 3000, respectively. Table V shows FS has better classification accuracy than other algorithms. The results on superpixels 500 and 1000 are better than the results on superpixels 3000.

The total accuracy with repeatedly running 50 on superpixels 500 and 1000 are represented by boxplots in Fig. 28.

Fig. 29 shows the classification results of San Francisco with

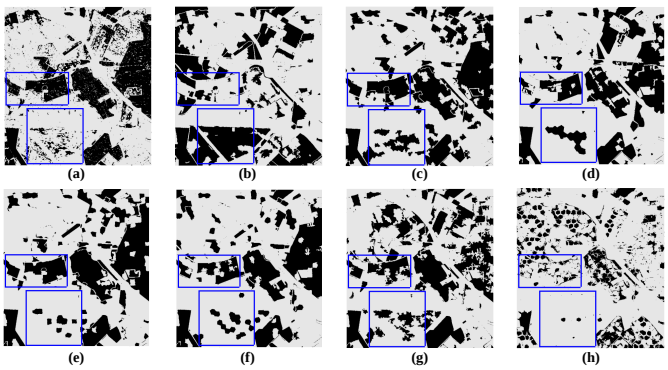


Fig. 26. Esar. The classification results.

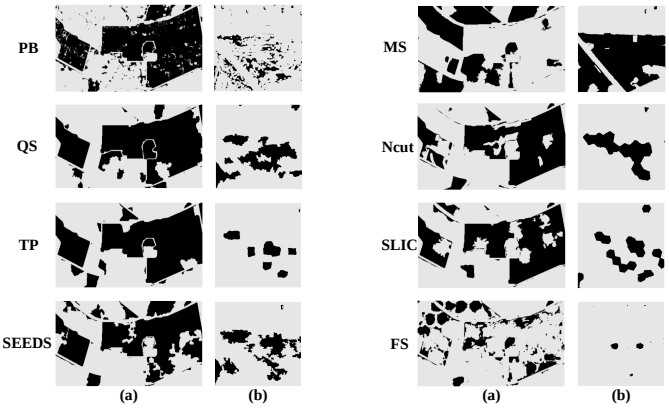


Fig. 27. Esar. The enlarged images of the selected regions.

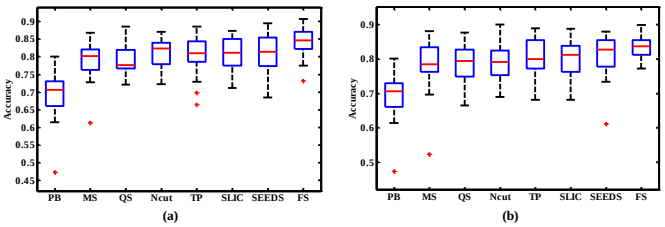


Fig. 28. SanFrancisco. (a) The number of superpixels is 500. (b) The number of superpixels is 1000.

500 superpixels. The enlarged images of the regions marked with blue rectangle are shown in Fig. 30.

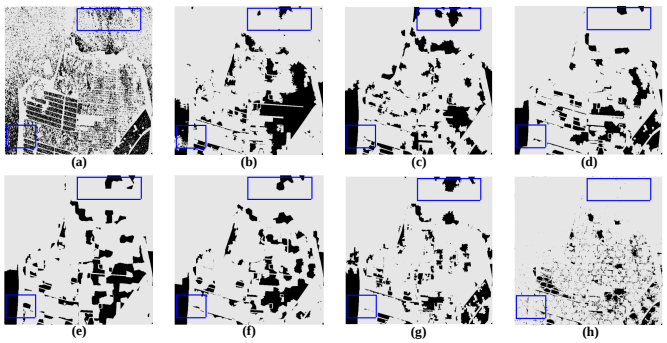


Fig. 29. SanFrancisco. The classification results.

According to the classification results on the three PolSAR

TABLE IV
ESAR. THE AVERAGE ACCURACY RATE AND STANDARD DEVIATION (STD) ACORSS 50 TESTS. THE BEST RESULT FOR EACH DATASET IS IN BOLD. (MEAN%±STD%)

| | PB | MS | QS | Ncut | TP | SLIC | SEEDS | FS |
|---|---|---|---|---|---|---|---|---|
| 500 | 65.59±6.2 | 60.81±9.9 | 57.95±8.1 | 63.65±9.4 | 64.38±7.8 | 62.96±7.7 | 65.15±9.7 | **69.33±5.9** |
| 1000 | 65.59±6.2 | 66.94±6.6 | 66.21±7.6 | 67.65±5.2 | 67.87±6.7 | 67.53±7.4 | 65.09±7.5 | **72.77±4.3** |
| 3000 | 65.59±6.2 | 65.05±8.7 | 67.36±5.0 | 65.70±6.9 | 65.48±7.0 | 65.27±6.7 | 64.87±7.8 | **71.25±5.7** |

TABLE V
SAN FRANCISCO. THE AVERAGE ACCURACY RATE AND STANDARD DEVIATION (STD) ACORSS 50 TESTS. THE BEST RESULT FOR EACH DATASET IS IN BOLD. (MEAN%±STD%)

| | PB | MS | QS | Ncut | TP | SLIC | SEEDS | FS |
|---|---|---|---|---|---|---|---|---|
| 500 | 68.81±6.1 | 78.94±5.2 | 78.51±4.0 | 81.02±3.8 | 80.55±5.3 | 81.02±5.0 | 81.21±5.0 | **84.21±3.9** |
| 1000 | 68.81±6.1 | 78.34±7.2 | 78.76±6.0 | 79.15±5.4 | 80.75±5.2 | 80.23±5.5 | 81.24±5.5 | **83.59±3.4** |
| 3000 | 68.81±6.1 | 76.28±3.6 | 76.06±5.5 | 77.01±4.8 | 76.75±4.9 | 77.87±5.2 | 80.11±5.3 | **81.85±3.4** |

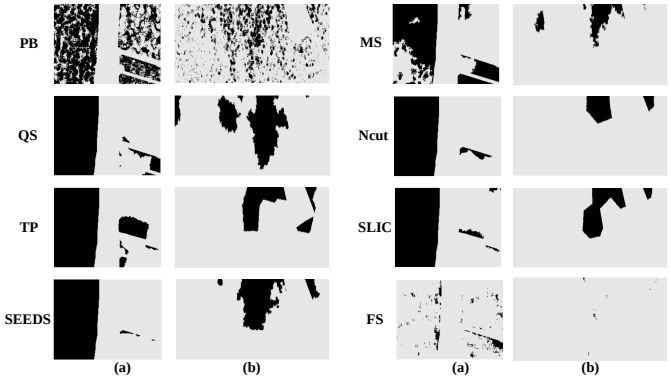


Fig. 30. SanFrancisco. The enlarged images of the selected region.

data set, the performance of FS based classification algorithm is discussed as follows.

(1) The classification accuracy of FS based algorithm are significant higher than that base on pixels (PB) and other superpixels algorithms.

(2) The number of superpixels is determined by the size and intrinsic complexity of the PolSAR image. If the number of superpixels is too small, it might cause under-segmentation in some area and the performance degradation of superpixels based algorithms and fuzzy-superpixels based algorithm. However, too many superpixles might cause that the performance of algorithms are sensitive to speckle noise.

### *E. Compared MAS_FS with MAS*

To further evaluate the performance of FS algorithm. FS is employed instead of superpixel algorithm in [21]. Fig. 31(a) shows the processing chain of algorithm MAS in [21]. MAS_FS denotes superpixels generation algorithm in MAS replaced by FS, the processing chain of which is represented in Fig. 31(b). Pixels are divided into two groups by FS, superpixels and undetermined pixels. For superpixels, the classification process is same with that in MAS. For undetermined pixels, a simple supervised classification process is adopted, which refers to Sec. IV(D). Briefly, superpixels with training pixels are assigned to the same label with the corresponding training pixels. Training set are expanded by superpixels. SVM is used to classify the undetermined pixels. The changing parts are shown in Fig. 31(b) with colors.

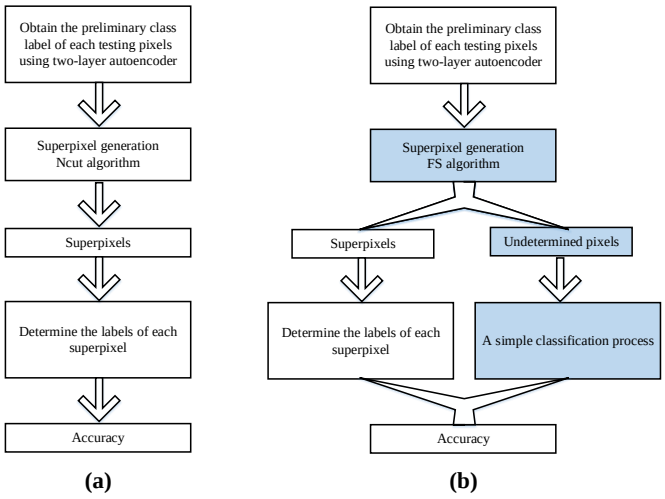


Fig. 31. The processing chains. (a) MAS. (b) MAS_FS.

The experiment is carried out on a subimage of Flevoland, as shown in Fig. 6. The number of superpixels is 200. The parameter S is set to 1/3, as in [21]. We choose about 0.2% training samples per class randomly and the remainder is the testing samples. The classification performance of two-layer autoencoders with different number of neurons is shown in Fig. 33. The range of the number of neurons is from 60 to 260. The FirLayer and SecLayer are the number of neurons at first and second layers, respectively. The best accuracy is obtained at FirLayer = 268 and SecLayer = 164, which is 72.55%.

Fig. 32 represents the accuracy as a function of the ratio of training samples per class, 0.2%, 1%, 5%, 10%, 20%. Different training sample ratio with different number of neurons for the best accuracy. From Fig. 32, we can see that the performance of algorithm MAS is further improved when superpixels algorithm used in MAS is replaced by FS.

The difference value between MAS and MAS_FS is shown in Fig. 32, from which we can see that FS has more significantly effects on algorithm when training samples ratio is small.

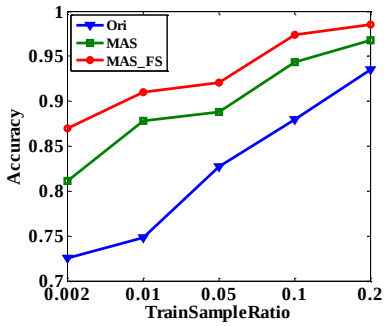


Fig. 32. Flevoland. The accuracy of the original two-layer autoencoder (Ori), MAS and MAS_FS.

### *F. Compared FS with HMRF*

First, hidden Markov random field (HMRF) is compared with superpixels. Second, the relationship between HMRF model and superpixels is discussed.

1) Comparison HMRF with superpixels.

HMRF algorithm proposed in [33] is used to segment the Flevoland dataset. The number of segmentation by HMRF is 6 (HMRF1, the number of classes in Flevoland dataset) and 200 (HMRF2, the same with the number of superpixels), respectively. The superpixels algorithms include MS, QS, SEEDS and FS. The number of generated superpixels is set to 200. The supervised classification process mentioned in Sec. IV (D) and (E) is employed to compute classification accuracy. The mean and standard deviation of accuracy are shown in Table VI.

TABLE VI
FLEVOLAND. THE CLASSIFICATION RESULTS WITH 200 SUPERPIXELS.

| MS | QS | SEEDS | HMRF1 | HMRF2 | FS |
|---|---|---|---|---|---|
| 80.79±5.6 | 79.48±9.4 | 83.31±5.0 | 64.14±6.9 | 79.77±3.9 | 86.70±3.2 |

From Table VI we can see that: (1) HMRF2 has comparable result with MS and QS algorithm; (2) HMRF1 and HMRF2 do not have superior classification accuracy than SEEDS and FS algorithm.

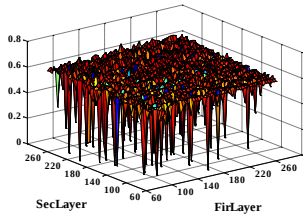


Fig. 33. Flevoland. The accuracy of two-layer autoencoders with different number of neurons.

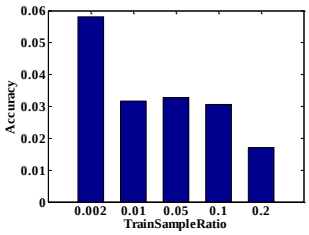


Fig. 34. Flevoland. The difference between MAS and MAS_FS.

The visual displays of the six classification results are shown in Fig. 35. The enlarged images of regions marked with blue rectangle are shown in Fig. 36.

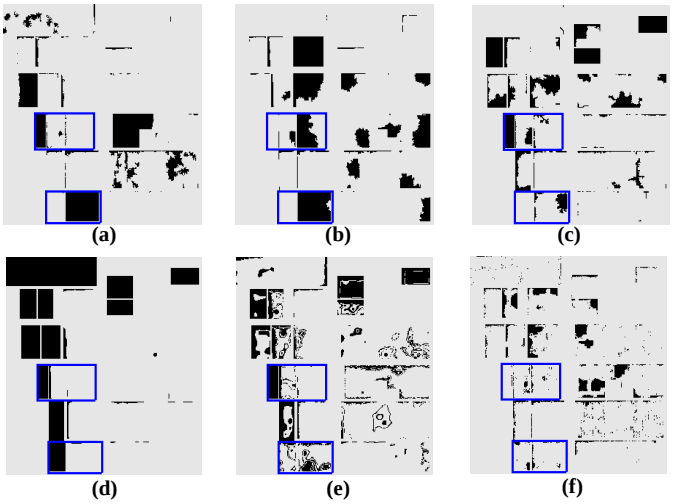


Fig. 35. Classification results. (a)-(f) are MS, QS, SEEDS, HMRF1, HMRF2 and FS, respectively.

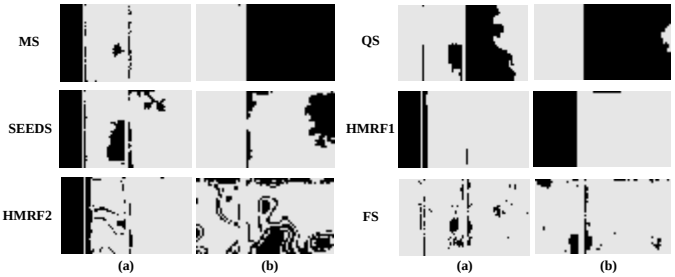


Fig. 36. The enlarged images of the selected regions.

2) Relationship between HMRF and superpixels.

Both superpixels and hidden Markov random field (HMRF) are for image segmentation. However, the relationship between superpixels and HMRF is not competitive but cooperative. A superpixel is a spatially-coherent, homogeneous, structure which preserves information over scales or sampling resolutions. Algorithms that over-segment the image are regarded as superpixel algorithms [34]. That is, many methods can be used to generate superpixels. HMRF model can be employed to segment image. MRF (or HMRF) based segmentation methods are very appealing for the reason that both prior knowledge and local spatial relationship are incorporated in MRF model [35]. However, the MRF model slow down as the number of nodes increases. The computationally efficiency of MRF model is low in large images when each pixel is a node. Besides, the pixel representation is often redundant, since the regions of interest is usually comprised of similar pixels [34]. Therefore, superpixel is used as basic unit of MRF instead of operating at the pixel level in many methods [36]–[41]. The advantage of integrating superpixel into MRF is that: (1) Enhance the computing efficiency; (2) Improve the segmentation result with structural information and similarities.

In this paper, revised fuzzy c-means (FCM) algorithm is used to generate fuzzy-superpixels. As mentioned in [34], [42], [43], FCM and HMRF are cooperative. In [42], FCM is employed to get the initial parameters of the mixture model (e.g. MRF). In [34], the MRF costs are designed to merge adjacent superpixels. Algorithm proposed in [43] deals with the HMRF model treatment problem as an FCM clustering problem, which combines the benefits of HMRF and FCM. Inspired by [44], FCM and HMRF can be combined to generate fuzzy superpixels in the future research.

## V. Conclusion

Superpixels have become a popular tool in image process field. Each superpixels algorithm has its own advantages that may be suitable for a particular application. A novel superpixels concept, named fuzzy-superpixels, is first proposed for image classification application. As mixed superpixels in superpixels have a bad effect on classification performance, thus the aim of fuzzy-superpixels is to generate less mixed superpixels (or more pure superpixels). In addition, a algorithm named FS is proposed to generate fuzzy-superpixels for PolSAR images. An empirical comparisons of FS with other superpixels algorithms are performed, concentrating on the three evaluation measures. In addition, a simple supervised classification experiment and a specially designed experiment are used to verify the performance of FS algorithm.

It is worth mentioning that a well-designed classification process can improve the performance of fuzzy-superpixels based image classification. Thus, the study on designing a more suitable classification process for fuzzy-superpixels should be concerned.

## Acknowledgment

The authors would like to thank the anonymous reviewers for their helpful comments and constructive suggestions for this paper.

## References

[1] Z. Wang, "Image segmentation by combining the global and local properties," *Expert Systems with Applications*, 2017.

[2] ——, "A new approach for robust segmentation of the noisy or textured images," *Siam Journal on Imaging Sciences*, vol. 9, no. 3, pp. 1409–1436, 2016.

[3] Z. Wang and Y. Yang, "A non-iterative clustering based soft segmentation approach for a class of fuzzy images," *Applied Soft Computing*, 2017.

[4] M. Van den Bergh, X. Boix, G. Roig, and L. Van Gool, "Seeds: Superpixels extracted via energy-driven sampling," *International Journal of Computer Vision*, vol. 111, no. 3, pp. 298–314, 2015.

[5] X. Boix, J. M. Gonfaus, J. V. D. Weijer, A. D. Bagdanov, and J. Serrat, "Harmony potentials," *International Journal of Computer Vision*, vol. 96, no. 1, pp. 83–102, 2012.

[6] J. Shen, Y. Du, W. Wang, and X. Li, "Lazy random walks for superpixel segmentation." *IEEE Transactions on Image Processing A Publication of the IEEE Signal Processing Society*, vol. 23, no. 4, pp. 1451–1462, 2014.

[7] R. Achanta, A. Shaji, K. Smith, A. Lucchi, and P. Fua, "Slic superpixels compared to state-of-the-art superpixel methods," *IEEE Transactions on Pattern Analysis and Machine Intelligence*, vol. 34, no. 11, pp. 2274–82, 2012.

[8] J. Shi and J. Malik, "Normalized cuts and image segmentation," *IEEE Transactions on Pattern Analysis and Machine Intelligence*, vol. 22, no. 8, pp. 888–905, 2000.

[9] L. Jiao and F. Liu, "Wishart deep stacking network for fast polsar image classification," *IEEE Transactions on Image Processing*, vol. 25, no. 7, pp. 1–1, 2016.

[10] H. Liu, D. Zhu, S. Yang, and B. Hou, "Semisupervised feature extraction with neighborhood constraints for polarimetric sar classification," *IEEE Journal of Selected Topics in Applied Earth Observations and Remote Sensing*, pp. 1–15, 2016.

[11] J. S. Lee, M. R. Grunes, and E. Pottier, "Quantitative comparison of classification capability: fully polarimetric versus dual and single-polarization sar," *Geoscience and Remote Sensing IEEE Transactions on*, vol. 39, no. 11, pp. 2343–2351, 2001.

[12] P. R. Kersten, J. S. Lee, and T. L. Ainsworth, "Unsupervised classification of polarimetric synthetic aperture radar images using fuzzy clustering and em clustering," *IEEE Transactions on Geoscience and Remote Sensing*, vol. 43, no. 3, pp. 519–527, 2005.

[13] S. Zhang, S. Wang, and L. C. Jiao, "New wishart mrf method for fully polsar image classification," *Computer Science*, vol. 41, no. 11, pp. 282–285,296, 2014.

[14] F. Liu, J. Shi, L. Jiao, H. Liu, S. Yang, J. Wu, H. Hao, and J. Yuan, "Hierarchical semantic model and scattering mechanism based polsar image classification," *Pattern Recognition*, vol. 59, no. C, pp. 325–342, 2016.

[15] X. Cheng, W. Huang, and J. Gong, "An unsupervised scattering mechanism classification method for polsar images," *IEEE Geoscience and Remote Sensing Letters*, vol. 11, no. 11, pp. 1677–1681, 2014.

[16] J. Zhang and D. Yan, "A supervised classification method of polarimetric sythetic aperture radar data using watershed segmentation and decision tree c5.0," *Geomatics and Information Science of Wuhan University*, vol. 39, no. 8, pp. 891–896, 2014.

[17] B. Zhang, G. R. Ma, L. Y. Lin, T. C. Mei, and Q. Q. Qin, "Classification of polarimetric sar images based on multi-scale markov random field," *Systems Engineering and Electronics*, vol. 33, no. 11, pp. 2413–2417, 2011.

[18] L. Zhao and E. Chen, "Segmentation and classification of polsar data using spectral graph partitioning," in *Eighth International Symposium on Multispectral Image Processing and Pattern Recognition*, 2013, pp. 2921–90.

[19] B. Liu, H. Hu, H. Wang, and K. Wang, "Superpixel-based classification with an adaptive number of classes for polarimetric sar images," *IEEE Transactions on Geoscience and Remote Sensing*, vol. 51, no. 2, pp. 907–924, 2013.

[20] J. Feng, Z. Cao, and Y. Pi, "Polarimetric contextual classification of polsar images using sparse representation and superpixels," *Remote Sensing*, vol. 6, no. 8, pp. 7158–7181, 2014.

[21] B. Hou, H. Kou, and L. Jiao, "Classification of polarimetric sar images using multilayer autoencoders and superpixels," *IEEE Journal of Selected Topics in Applied Earth Observations and Remote Sensing*, vol. 9, no. 7, pp. 1–10, 2016.

[22] J. Li, H. Zhang, and L. Zhang, "Efficient superpixel-level multitask joint sparse representation for hyperspectral image classification," *IEEE Transactions on Geoscience and Remote Sensing*, vol. 53, no. 10, pp. 1–14, 2015.

[23] L. Vincent and P. Soille, "Watersheds in digital spaces: An efficient algorithm based on immersion simulations," *IEEE Transactions on Pattern Analysis and Machine Intelligence*, vol. 13, no. 6, pp. 583–598, 1991.

[24] K. Fu, C. Gong, Y. H. Gu, and J. Yang, "Normalized cut-based saliency detection by adaptive multi-level region merging," *IEEE Transactions on Image Processing*, vol. 24, no. 12, p. 5671, 2015.

[25] D. Comaniciu and P. Meer, "Mean shift: a robust approach toward feature space analysis," *IEEE Transactions on Pattern Analysis and Machine Intelligence*, vol. 24, no. 5, pp. 603–619, 2002.

[26] A. Vedaldi and S. Soatto, *Quick Shift and Kernel Methods for Mode Seeking*, 2008.

[27] A. Levinshtein, A. Stere, K. N. Kutulakos, D. J. Fleet, S. J. Dickinson, and K. Siddiqi, "Turbopixels: fast superpixels using geometric flows." *IEEE Transactions on Pattern Analysis and Machine Intelligence*, vol. 31, no. 12, pp. 2290–2297, 2009.

[28] J. C. Bezdek, R. Ehrlich, and W. Full, "Fcm: The fuzzy c-means clustering algorithm," *Computers and Geosciences*, vol. 10, no. 2-3, pp. 191–203, 1984.

[29] F. Qin, J. Guo, and F. Lang, "Superpixel segmentation for polarimetric sar imagery using local iterative clustering," *IEEE Geoscience and Remote Sensing Letters*, vol. 12, no. 1, pp. 13–17, 2015.

[30] J. S. LEE, M. R. GRUNES, and R. KWOK, "Classification of multi-look polarimetric sar imagery based on complex wishart distribution," in *Telesystems Conference, 1992. NTC-92., National*, 1994, pp. 7/21–7/24.

[31] A. Yu, P. Qin, "Unsupervised polarimetric sar image segmentation and classification using region growing with edge penalty," *IEEE Transactions on Geoscience and Remote Sensing*, vol. 50, no. 4, pp. 1302–1317, 2012.
[32] S. Uhlmann and S. Kiranyaz, "Integrating color features in polarimetric sar image classification," *IEEE Transactions on Geoscience and Remote Sensing*, vol. 52, no. 4, pp. 2197–2216, 2014.
[33] Q. Wang, "Hmrf-em-image: Implementation of the hidden markov random field model and its expectation-maximization algorithm," *Computer Science*, vol. 94-b, no. 1, pp. 222–233, 2012.
[34] A. P. Moore, S. J. D. Prince, J. Warrell, U. Mohammed, and G. Jones, "Superpixel lattices," in *Computer Vision and Pattern Recognition, 2008. CVPR 2008. IEEE Conference on*, 2008, pp. 1–8.
[35] X. F. Wang and X. P. Zhang, "A new localized superpixel markov random field for image segmentation," in *IEEE International Conference on Multimedia and Expo*, 2009, pp. 642–645.
[36] S. Li, X. Jia, and B. Zhang, "Superpixel-based markov random field for classification of hyperspectral images," in *Geoscience and Remote Sensing Symposium*, 2014, pp. 3491–3494.
[37] A. Schick, M. Bauml, and R. Stiefelhagen, "Improving foreground segmentations with probabilistic superpixel markov random fields," in *Computer Vision and Pattern Recognition Workshops*, 2012, pp. 27–31.
[38] M. Ye, Z. Cao, Z. Yu, and X. Bai, "Crop feature extraction from images with probabilistic superpixel markov random field," *Computers and Electronics in Agriculture*, vol. 114, no. C, pp. 247–260, 2015.
[39] T. Hamedani, R. Zarei, and A. Harati, "Superpixel based rgb-d image segmentation using markov random field," in *International Symposium on Artificial Intelligence and Signal Processing*, 2015, pp. 89–94.
[40] J. Wang and S. K. Yeung, "Superpixelizing binary mrf for image labeling problems," *Computer Science*, 2015.
[41] X. Wang, G. Yan, H. Wang, J. Fu, J. Hua, J. Wang, Y. Yang, G. Zhang, and H. Bao, "Semantic annotation for complex video street views based on 2d3d multi-feature fusion and aggregated boosting decision forests," *Pattern Recognition*, vol. 62, no. C, pp. 189–201, 2017.
[42] Y. Hou, Y. Yang, N. Rao, X. Lun, and J. Lan, "Mixture model and markov random field-based remote sensing image unsupervised clustering method," *Opto-Electronics Review*, vol. 19, no. 1, pp. 83–88, 2011.
[43] S. P. Chatzis and T. A. Varvarigou, "A fuzzy clustering approach toward hidden markov random field models for enhanced spatially constrained image segmentation," *IEEE Transactions on Fuzzy Systems*, vol. 16, no. 5, pp. 1351–1361, 2008.
[44] S. P. Awate, H. Zhang, and J. C. Gee, "A fuzzy, nonparametric segmentation framework for dti and mri analysis: with applications to dti-tract extraction." in *Biennial International Conference on Information Processing in Medical Imaging*, 2007, pp. 296–307.

**Yuwei Guo** was born in China in 1988. She received the Ph.D. degrees in circuits and systems form Xidian University, Xi'an, China, in 2017. Currently, she is a lecturer in Key Laboratory of Intelligent Perception and Image Understanding of Ministry of Education, International Research Center for Intelligent Perception and Computation, Joint International Research Laboratory of Intelligent Perception and Computation, School of Artificial Intelligence, Xidian University, Xi'an, China.

Her research interests include rough set theory, data mining, deep learning and image classification.

**Licheng Jiao** (F'17) received the B.S. degree from Shanghai Jiao Tong University, Shanghai, China, in 1982 and the M.S. and Ph.D. degrees from Xi'an Jiaotong University, Xi'an, China, in 1984 and 1990, respectively. Since 1992, he has been a Professor with the School of Electronic Engineering, Xidian University, Xi'an, where he is currently the Director of the Key Laboratory of Intelligent Perception and Image Understanding of the Ministry of Education of China, International Research Center of Intelligent Perception and Computation. His current research interests include intelligent information processing, image processing,machine learning, and pattern recognition. Prof. Jiao was a recipient of the Second Prize of the National Natural Science Award in 2013.

**Shuang Wang** (M'07), was born in Shannxi, China, in 1978. She received the B.S., M.S., and Ph.D. degrees in circuits and systems form Xidian University, Xi'an, China, in 2000 and 2003, respectively. Currently, she is a Professor in the Key Laboratory of Intelligent Perception and Image Understanding of Ministry of Education of China, Xidian University. Her main research interests are Sparse Representation, image processing and high-resolution SAR image processing.

**Shuo Wang** is a Research Fellow at the Centre of Excellence for Research in Computational Intelligence and Applications (CERCIA) in the School of Computer Science, the University of Birmingham (UK). She received the Ph.D. degree in Computer Science from the University of Birmingham, U.K., in 2011, sponsored by the Overseas Research Students Award (ORSAS) from the British Government (2007). Her research interests include class imbalance learning, ensemble learning, online learning and machine learning in software engineering. Her work has been published in internationally renowned journals and conferences.

**Fang Liu** (SM'07) received the B.S. degree from Xi'an Jiaotong University, Xi'an, China, in 1984, and the M.S. degree from Xidian University, Xi'an, in 1995, both in computer science and technology. She is currently a Professor with Xidian University. She has authored or co-authored five books and over 80 papers in journals and conferences. Her current research interests include image perception and pattern recognition, machine learning, and data mining. Prof. Liu was a recipient of the Second Prize of the National Natural Science Award in 2013.

**Wenqiang Hua** Wenqiang Hua received the B.E degree from theUniversity of Electronic Science and Technology of China, Chengdou, China, in 2012. He is currently working toward the Ph.D. degree in the Key Laboratory of Intelligent Perception and Image Understanding of Ministry of China, Xidian University, Xi'an, China. His main research interests is PolSAR image processing.